Earth Reinforcement, Ochiai, Yasufuku & Omine (eds) © 1996 Balkema, Rotterdam. ISBN 9054108339

Internal stability analysis and deformation prediction for fabric reinforced earth structure

H.T.Kim
Department of Civil Engineering, Hong-Ik University, Seoul, Korea

E.S.Lee
E & S Engineering Co., Ltd, Seoul, Korea

I.K.Kang
VNIEL Consultants Co., Ltd, Seoul, Korea

Y.K.Bang
Department of Civil Engineering, Dae-Won Jr College, Jechun, Korea

ABSTRACT : In the present paper internal design method relating to the use of fabric reinforcements in reinforced earth structures for both stress and strain considerations are presented. The soil-reinforcement interaction is modeled by relating nonlinear elastic soil behavior to nonlinear response of the fabric reinforcement. For purposes of assessing the strain behavior of the fabric reinforcements, nonlinear elastic model of hyperbolic form describing the load-extension relation of fabrics is employed. An attempt to define the improvement in bond-linkage at the interconnecting nodes of the fabric reinforced earth structure due to the confining stress is further made. Good predictive capability of the proposed method of analysis is demonstrated by comparisons with data for test walls for which measured values of reinforcement tensions and deformations are available. Results of analytical parametric study are also included.

1 INTRODUCTION

The use of fabrics as reinforcing elements for reinforced earth construction appears to have several advantages including lower cost, light weight, improved durability, high frictional characteristics, and ease of storage, handling and transportation.

Current design methods for reinforced earth structures take no account of the magnitude of the strains induced in the tensile members as these are invariably manufactured from high modulus materials, such as steel, where strains are unlikely to be significant. With fabrics, however, large strains may frequently be induced and it is important to determine these to enable the stability of the structure to be assessed.

In the present paper internal design method relating to the use of fabric reinforcements in reinforced earth structures for both stress and strain considerations are presented. For the internal stability analysis against rupture and pullout of the fabric reinforcements, a strain compatibility analysis procedure that considers the effects of reinforcement stiffness, relative movement between the soil and reinforcements, and compaction-induced stresses as studied by Ehrlich & Mitchell(1994) is used. However, the soil-reinforcement interaction is modeled by relating nonlinear elastic soil behavior to nonlinear response of the fabric reinforcement. The soil constitutive model used is a modified version of the hyperbolic soil model and compaction stress model proposed by Duncan et al.(1980,1986), and iterative step-loading approach is used to take nonlinear soil behavior into consideration.

For purposes of assessing the strain behavior of the fabric reinforcements, nonlinear elastic model of hyperbolic form describing the load-extension relation of fabrics is employed. A procedure for specifying the strength characteristics of paraweb multicord manufactured by vacuum die coating yarns of polyester with a sheath of black polyethylene as well as needle punched non-woven geotextile made from infinite polyester fibres is also described which may provide a more convenient procedure for incorporating the fabric properties into the prediction of fabric deformations. An attempt to define the improvement in bond-linkage at the interconnecting nodes of the fabric reinforced earth structure due to the confining stress is further made.

2 SOIL-REINFORCEMENT INTERACTION

Fabric reinforcement is modeled as a nonlinear material with perfect interface adherence to the adjacent soil at the point of maximum tension. This means that there is no slip between the soil and the reinforcements; the soil and reinforcement strains are the same at this interface. It is assumed that each reinforcement layer is responsible for local horizontal equilibrium of the corresponding horizontal slices of the active zone of thickness(s_v) and transverse width(s_h), where s_v and s_h are the vertical and horizontal spacings between reinforcements, respectively(Fig. 1). This condition means that

$$T_{max} - s_h s_v (\sigma_h)_{ave} = 0 \quad (1)$$

in which T_{max} = maximum reinforcement tension and $(\sigma_h)_{ave}$ = average horizontal soil stress.

The maximum tension T_{max} in any reinforcement layer can be determined for the final condition at the end of construction using

$$T_{max} = S_v S_h \sigma_{xr} = S_v S_h K_r \sigma_z \quad (2)$$

in which σ_z= vertical stress in the soil at the point of maximum tension in the reinforcement at the soil-reinforcement interface, and K_r = corresponding residual lateral earth pressure coefficient at the end of construction.

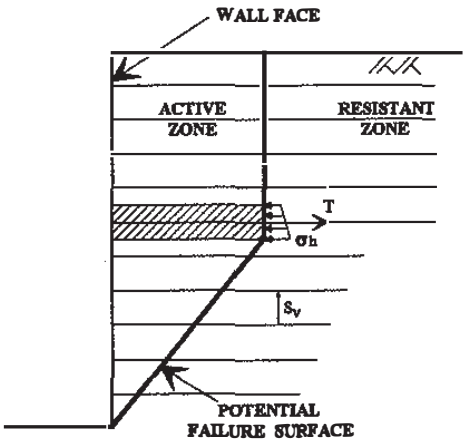

Fig. 1 Equilibrium Condition

2.1 Determination of K_r

For a modeling of nonlinear behavior of fabric reinforcement the simplest form of hyperbolic relation capable of describing the load-extension relation of fabric is adopted. An additional benefit is that it may also be possible to specify the required fabric properties more realistically. The maximum fabric reinforcement tension T_{max} is therefore related to the corresponding strain ε_{xr} by

$$T_{max} = \frac{\varepsilon_{xr}}{(\alpha_1 m)\varepsilon_{xr} + (\alpha_2 c)} \quad (3)$$

where m and c are hyperbolic constants describing the stress-strain relation of fabric reinforcement. m represents inverse of the ultimate strength of the fabric reinforcement and c represents slope of load-extension relation at origin, respectively. And also α_1 and α_2 are parameters at corresponding depth defining the confining effects imposed on the fabric reinforcement by the surrounding soils.

The assumption of perfect soil-reinforcement interface adherence at the location of maximum reinforcement tension means

$$\varepsilon_{xr} = \varepsilon_{xs} \quad (4)$$

Developed soil strains ε_{xs} for loading and unloading in the reinforcement direction at the soil-reinforcement interface are determined based on incremental elasticity under plane strain conditions and hyperbolic formulation of tangent modulus proposed by Duncan et al. Assuming that the horizontal stress σ_x at this interface point is equal to the average horizontal stress $(\sigma_h)_{ave}$(Fig. 1),

$$\sigma_x = (\sigma_h)_{ave} \quad (5)$$

Rearrangement of Eqs. (1) and (3) ~ (5) with developed soil strains ε_{xs} gives Eq. (6) for loading and Eq. (7) for unloading.

$$1.0 = \alpha_1 m s_h s_v K_c \sigma_{zc} + \alpha_2 c s_h s_v \frac{A_2}{A_1} \quad (6)$$

in which $A_1 = (1 - \nu_0^2)(1 - K_{aa})^2 (K_0 - K_c) K_0$, $A_2 = kP_a \left(\frac{\sigma_{zc}}{P_a}\right)^n (K_c - K_{aa})(K_0 - K_{aa})$, K_c =lateral earth pressure coefficient during compaction, and σ_{zc} = maximum past equivalent vertical stress including compaction at the given depth.

$$1.0 = \alpha_1 m s_h s_v (K_c \sigma_{zc} - K_r \sigma_z) - \alpha_2 c s_h s_v \left(\frac{B_2}{B_1}\right) \quad (7)$$

in which

$B_1 = (1 - \nu_{ur}^2)\{(K_c - K_{d2}) OCR - (K_r - K_{d2})\}$

$B_2 = k_u P_a \left(\frac{\sigma_{xr}}{P_a}\right)^n (K_c \cdot OCR - K_r)$, and K_{aa}=equivalent active Rankine earth pressure coefficient, k, k_u and n = Duncan et al.'s modulus number for loading, unloading and modulus exponent, respectively, P_a = atmospheric pressure, and the overconsolidation ratio OCR is

$$OCR = \sigma_{zc} / \sigma_z \quad (8)$$

Poisson's ratio for unloading at rest is given by

$$\nu_{ur} = K_{d2} / (1 + K_{d2}) \quad (9)$$

in which

$$K_{d2} = K_0 (OCR - OCR^{\beta}) / (OCR - 1) \quad (10)$$

where K_{d2} is the at rest decremental lateral earth pressure coefficient for unloading. The unloading coefficient β can be related to sin ϕ and estimated by

$$\beta = 0.7 \sin\phi \quad (11)$$

Corresponding residual lateral earth pressure coefficient at the end of construction K_r is finally determined by trial using Eqs. (6) and (7) as previously described. The residual horizontal soil stress σ_{xr} is also related to the vertical stress σ_z by

$$\sigma_{xr} = K_r \sigma_z \quad (12)$$

The maximum reinforcement tension T_{max} expressed previously by Eq. (2) is finally determined using Eqs. (1), (5) and (12).

2.2 Strains in fabric reinforcement on the basis of nonlinear relation

Considering the extension of the fabric reinforcement when subject to an hyperbolic stress-strain relation, the tension T_x expected in the reinforcement at distance x from the facing is estimated by assuming a simple linear variation along the length of reinforcement as follows:

$$T_x = T_{max} \frac{(1-\rho)x}{(L-L')} + T_{max} \cdot \rho \quad (0.0 < x \leq L-L' \ case) \quad (13\text{-}1)$$

$$T_x = T_{max} \frac{(L-x)}{L'}, \ (L-L' < x < L \ case) \quad (13\text{-}2)$$

in which L' = effective length of reinforcement located outside the active zone and the stress-strain relation is given by Eq. (3), and ρ is a parameter to define the magnitude of reinforcement tension expected at the facing.

The total extension δ_L over a length of fabric reinforcement L is therefore given by

$$\delta_L = -\frac{c}{m}(L-L') + \frac{DF+EG}{D^2}\{\ln G - \ln(DL'-DL+G)\} - \frac{c}{m}L' - \ln(1-T_{max}\,m)\frac{L'c}{m^2 T_{max}} \quad (14)$$

in which

$$D = m T_{max} \frac{(1-\rho)}{(L-L')}, \ E = c T_{max} \frac{(1-\rho)}{(L-L')},$$

$$F = c T_{max} \rho, \text{ and } G = 1 - m T_{max} \rho.$$

2.3 Seepage pressures along the failure surface

Based on the Gray's seepage theory(1958), seepage pressures expected along the bilinear failure surface are estimated(Fig. 2). Expression derived in the present study for a estimation of seepage force P_{w1} is given below.

$$P_{w1} = \frac{1}{2}\gamma_w H^2 \left[\left(\frac{H_a}{H}\right)^2 + \frac{32}{\pi^3} \sum_{m=0}^{\infty} \frac{(-1)^m}{(2m+1)^3} e^{-(2m+1)\frac{\pi l}{2H}} \times \left\{ \cos\left((2m+1)\frac{\pi H_a}{2H}\right) - 1 \right\} \right] \quad (15)$$

Seepage force P_{w2} is similarly determined and the expression for P_{w2} is omitted here due to a limited spacing.

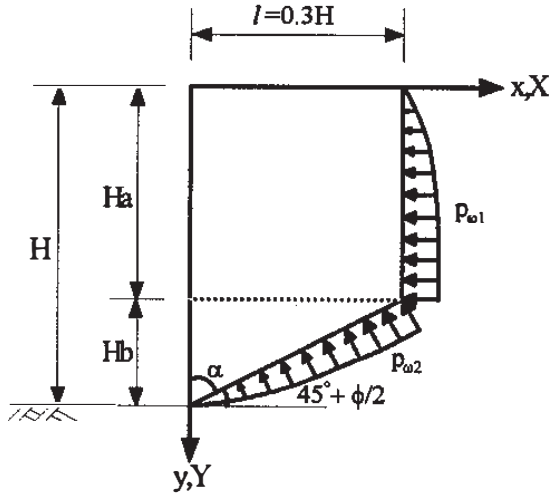

Fig. 2 Seepage Pressures

2.4 Analyses of typical strength characteristics of the fabric reinforcements

Typical hyperbolic constants of m and c defined previously in Eq. 3 are estimated by regression analyses of the load-extension test results for paraweb multicord manufactured by vacuum die coating yarns of polyester with a sheath of black polyethylene and needle punched non-woven geotextile made from infinite polyester fibres. The results of analyses are illustrated in Figs. 3 and 4, respectively.

3 COMPARISION WITH MEASUREMENTS

The main objectives of this study are to estimate maximum reinforcement tensions and facing lateral

deformations using the proposed procedure, and to see how well these predictions compare with the measured values.

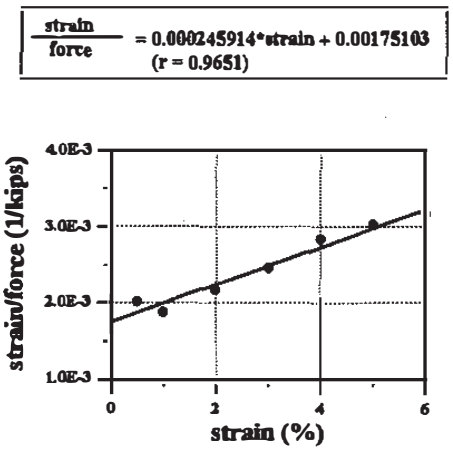

Fig. 3 Stress-Strain Relation(Paraweb Multi-cord)

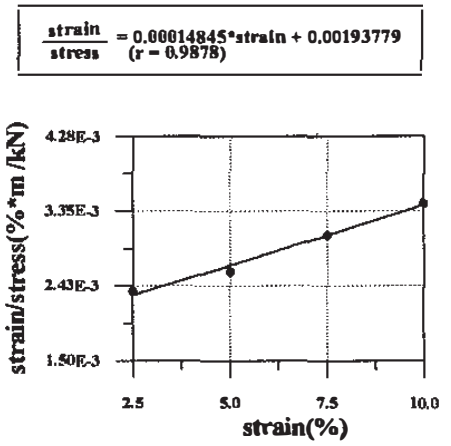

Fig. 4 Stress-Strain Relation(Non-Woven Geo-textile)

3.1 Comparison 1

The results from the proposed method of analysis are compared with test measurements reported by Ho & Rowe(1993). The height H of reinforced soil wall was 6 m constructed with cohesionless fill with a level surface and reinforced with 6 layers of sheet-like geosynthetic reinforcement. The length L of each layer was 4.25 m with a typical L/H ratio of 0.71, and no surcharge loading on the top surface was applied.

Fig. 5 shows the relationship between maximum reinforcement tension per linear meter of wall T_{max} along the height above base of wall, as determined from instrumentation and predicted by analyses using the proposed method. This result shows that, except for the lowest reinforcement layer, agreement between the measurements and predictions is good. Similar to most field observations, at upper levels the magnitude of the maximum tension exceed that given by Rankine's active condition or even the at rest condition; while at lower levels, the magnitude of the maximum tension is relatively less. This is because the foundation provides significant horizontal restraint to lateral deformation of the backfill at the backfill-foundation interface. The horizontal restraint modifies the stress condition near the bottom of the wall and the assumed hypothesis of $\tau_{xz} = 0$ is not valid at this level. The proposed method of analysis does not take this restraint into account.

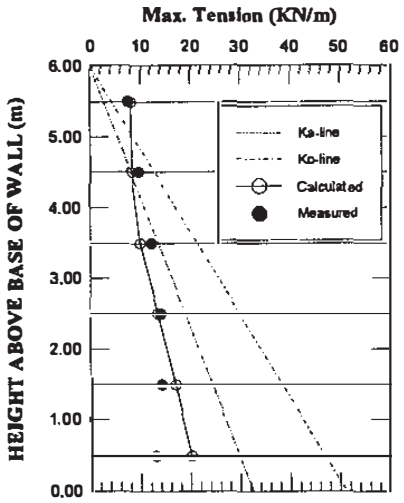

Fig. 5 Maximum Tension Comparision

Hyperbolic load-extension relation of needle punched non-woven geotextile up to 10% of axial strain(see Fig. 4) was used in this analysis. Also values of the parameter α_1(refer to Eq. 3) were assumed to be constant irrespective of reinforcement levels, whereas values of α_2 were assumed to vary linearly from 1.0 at the top to 0.2 at the lowest level.

3.2 Comparison 2

Balzer et al.(1990) reported the results of one set of full scale tests to study the performance of geotextile reinforced abutment built according to the French procedure. A needle punched non-woven polyester geotextile was used as reinforcement layers. The full scale abutment structure with a total height of 2.88 m had five geotextile reinforcement layers, each approximately 0.50 m in height. The geotextile was wrapped around to form an almost vertical wrapped-around wall face. The effective length of reinforcement was 2 m. The tensile modulus of the geotextile was estimated to be about 0.32 ~ 0.64 KN/m from unconfined stress-strain tests. The fill material used was gravelly sand with a friction angle of 39° .

The full scale test abutment was subjected to a loading and unloading cycle until about 110 KN was reached. This corresponds to a strip load of 62 KN/m over a 0.9 m width. Then the loading were increased stepwise until

failure occurred at about 640 KN.

Figs. 6 ~ 8 show the detailed comparisons of measured and predicted lateral deformations along the height above base of wall at various concentrated strip loading conditions. Overall, the proposed deformation evaluation procedure gives very comparable results, generally within 13%(1.71mm) ~ 29%(1.87mm) of the measured deformations at wall facing.

Hyperbolic load-extension relation of needle punched non-woven geotextile and values of the parameters α_1, α_2 applied to this analysis are the same as those in Comparison 1.

4 PARAMETRIC STUDY

An analytical parametric study was made to investigate the effect and significance of compaction induced stress and other pertinent parameters on the developments of

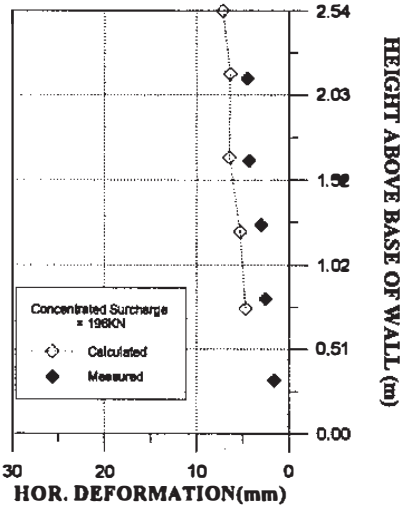

Fig. 6 Deformation Comparision 1

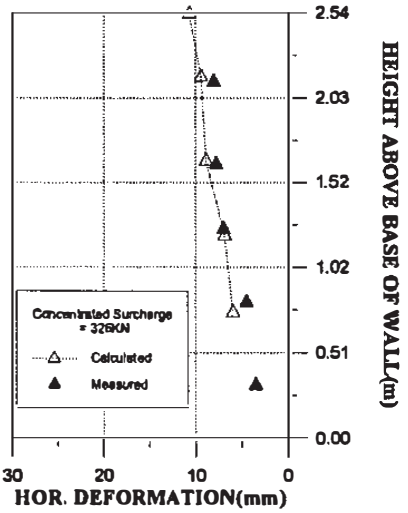

Fig. 7 Deformation Comparision 2

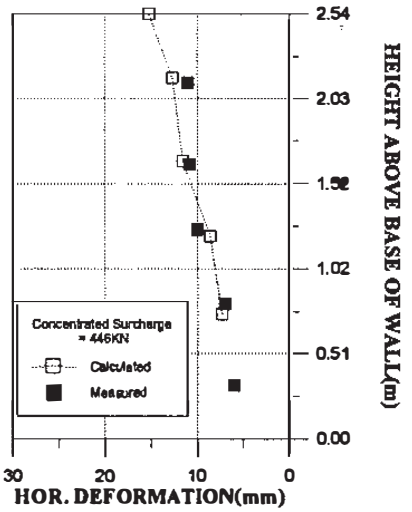

Fig. 8 Deformation Comparision 3

residual lateral earth pressure coefficient and wall facing lateral deformation at the end of construction. The compaction equipment considered in this study was equivalent to the Dynapac CA25 vibratory roller with a maximum vertical operating drum force Q of 160 KN and length of 2.1 m. Paraweb multicords manufactured by vacuum die coating yarns of polyester with a sheath of black polyethylene were adopted as reinforcing material. Detailed parameters, including typical nonlinear soil properties, used in this study are described in Table 1. Hyperbolic load-extension relation of paraweb multicord up to 6% of axial strain was previously analyzed from experimental test results and given in Fig. 3.

Table 1. Parameters used in parametric study

$\phi=40°$, $\gamma_t=2.1t/m^3$, $H=7.501m$
$L=7.50$(top reinf.) ~4.44(bottom reinf.)
$k=2000$, $k_u=2120$, $n=0.54$, $R_f=0.91$
$s_v = s_h = 0.75m$, $\alpha_1=1.0$

Fig. 9 shows the corresponding residual lateral earth pressure coefficient at the end of construction K_r, as determined by analyses using the proposed method. This study clearly exemplifies the importance of the compaction effects. Compaction stresses strongly influence the K_r values from the wall top to a depth of about 4.0 m, which is similar to most field observations as reported by Ehrlich & Mitchell(VSL wall at Hayward, Calif., and two reinforced earth walls, one at the FHWA test site in Illinois and one at WES). The K_r values in all the reinforcement layers above this depth are higher than K_0, which is the limiting condition for no compaction of backfill. At greater depths, the overburden stresses exceed the compaction-induced stresses, and the mobilized

average K_r is close to K_0 due to the high relative soil-reinforcement stiffness.

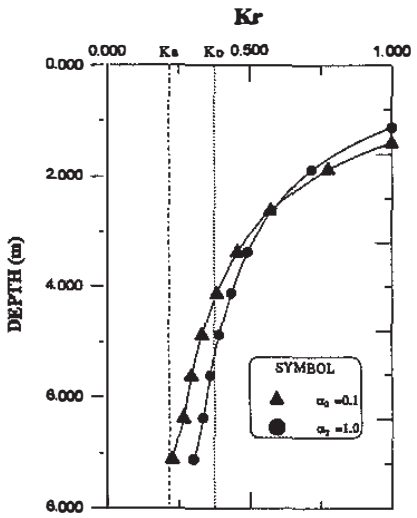

Fig. 9 Analysis of K_r - values

Fig. 10 shows the distribution of lateral deformations expected at the wall facing reinforced with paraweb multicords, as determined by the proposed evaluation procedure. It could be realized from the results of Fig. 10 that seepage pressures along the failure surface as well as parameter α_2 representing the initial slope of load-extension hyperbolic relation of reinforcing material greatly affect the development of lateral deformations. The maximum values of lateral deformations vary in the range of 1 ~ 10 mm according to the effect of seepage pressures and the magnitude of parameter α_2. It is also realized that the maximum lateral deformation is in general expected to occur in the middle height of the wall for the case analyzed here.

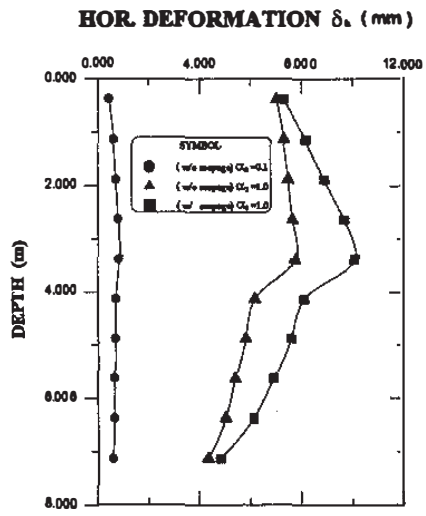

Fig. 10 Analyses of Deformations

5 CONCLUSIONS

For the internal stability analysis against rupture and pullout of the fabric reinforcements, in the present paper a strain compatibility analysis procedure that considers the effects of reinforcement stiffness, relative movement between the soil and reinforcements, and compaction-induced stresses as studied by Ehrlich and Mitchell is used. However, the soil-reinforcement interaction is modeled by relating nonlinear elastic soil behavior to nonlinear response of the fabric reinforcement. The soil constitutive model used is a modified version of the hyperbolic soil model and compaction stress model proposed by Duncan et al., and iterative step-loading approach is used to take nonlinear soil behavior into consideration.

For purposes of assessing the strain behavior of the fabric reinforcements, nonlinear elastic model of hyperbolic form describing the load-extension relation of fabrics is employed. A procedure for specifying the strength characteristics of paraweb multicord manufactured by vacuum die coating yarns of polyester as well as needle punched non-woven geotextile is also described which may provide a more convenient procedure for incorporating the fabric properties into the prediction of fabric deformations. An attempt to define the improvement in bond-linkage at the interconnecting nodes of the fabric reinforced earth structure due to the confining stress is further made.

Good predictive capability of the proposed method of analysis is demonstrated by comparisons with data for test walls for which measured values of reinforcement tensions and deformations are available. Results of analytical parametric study for the case of a wall reinforced with paraweb multicords are also included.

REFERENCES

Balzer, E., Matichard Y. and Thamm, B.R. 1990, Geotextile reinforced abutment: full scale test and theory, Performance of reinforced soil structures, British Geotechnical Society, pp. 47~52.

Duncan, J.M. and Seed, R.B. 1986, Compaction-induced earth pressure under K_0-conditions, ASCE, Journal of Geotechnical Engineering, Vol. 112, No. 1, pp. 1~22.

Duncan, J.M., Byrne, P., Wong, K.S., and Mabry, P. 1980, Strength, stress-strain and bulk modulus parameters for finite element analyses of stresses and movements in soil masses, Geotechnical Engineering Research Report No. UCB/GT/80-01, Univ. of Calif., Berkeley.

Ehrlich, M. and Mitchell, J.K. 1994, Working stress design method for reinforced soil walls, ASCE, Journal of Geotechnical Engineering, Vol. 120, No. 4, pp. 625~645. And Discussion by Neely, W.J.(1995).

Gray, H. 1958, Contribution to the analysis of seepage effects in backfills, Geotechnique, Vol. 8, No. 4, pp. 166 ~170.

Ho, S.K. and Rowe, R.K. 1993, Finite element analysis of geosynthetics-reinforced soil walls, Geosynthetics'93 - Vancouver, Canada, pp. 203~216.